Deformation Analysis of Micro-Sized Material Using Strain Gradient Plasticity

S. M. Byon
Rolling Technology and Process Control Research Group, POSCO Technical Research Laboratories, Pohang, Korea
Youngseog Lee*
Department of Mechanical Engineering, Chung-Ang University, Seoul 156-756, Korea

To reflect the size effect of material (1~15 μm) during plastic deformation of polycrystalline copper, a constitutive equation which includes the strain gradient plasticity theory and intrinsic material length model is coupled with the finite element analysis and applied to plane strain deformation problem. The method of least square has been used to calculate the strain gradient at each element during deformation and the effect of distributed force on the strain gradient is investigated as well. It shows when material size is less than the intrinsic material length (1.54 μm), its deformation behavior is quite different compared with that computed from the conventional plasticity. The generation of strain gradient is greatly suppressed, but it appears again as the material size increases. Results also reveal that the strain gradient leads to deformation hardening. The distributed force plays a role to amplify the strain gradient distribution.

Key Words: Micro Forming, Intrinsic Material Length, Strain Gradient Plasticity, Constitutive Equation, Finite Element Analysis

1. Introduction

Recently, there have been many investigations regarding plastic deformation behavior of material when its physical size scales down from tens of microns to fraction of microns. As its size becomes small to such extent, stress at a point is related to strain at the point and that in the neighborhood of the point. The strain in the neighborhood of the point is linked to the spatial gradient of strain, i.e., strain gradient. The stress at a point increases owing to the strain gradient (Nix, 1989; Stelmashenko et al., 1993; Fleck et al., 1994; Ma and Clarke, 1995; McElhaney et al., 1998; Stolken and Evans, 1998).

From the micro-mechanics viewpoint, this phenomenon is attributable to the distribution of dislocation density. When material is deformed plastically, inhomogeneous dislocations exist as a diverse form in the material. According to its origination, it can be divided into two types of dislocations, i.e., statistically stored dislocation (SSD) and geometrically necessary dislocations (GND) (Ashby, 1970; Arsenlis and Park, 1999).

Hutchinson (Fleck and Hutchinson, 1993; 1997) reported that as a region where deformation occurs or material size itself becomes very small, the GND relative to the SSD increases. GND is in connection with the gradient of plastic strain because the dislocation plays a role to keep the compatibility of points (particles) undergoing a local deformation. The theory that takes the strain gradient into account is called the strain gradient plasticity. On the other hand SSD is related with plastic strain at continuum level since dislocation

* Corresponding Author,
E-mail: ysl@cau.ac.kr
TEL: +82-2-820-5256; **FAX**: +82-2-814-9476
Department of Mechanical Engineering, Chung-Ang University, Seoul 156-756, Korea. (Manuscript **Received** August 17, 2005; **Revised** February 24, 2006)

is distributed randomly in the statistical aspect. If the material size increases, SSD becomes large relatively compared with GND. Therefore, the effect of strain gradient is negligible.

Research groups (Nix and Gao, 1998 ; Gao et al., 1999 ; Huang et al., 2000a ; 2000b ; 2004 ; Qiu et al., 2003) modeled GND mathematically and expressed it in terms of strain gradient and consequently could examine the effect of GND quantitatively upon deformation. Thus, through incorporating this model with continuum mechanics, they opened the way for the plastic deformation analysis of micro-sized material. This approach might be applied to the analysis of micro-forming, micro-machining and residual stress analysis of micro-electronic packaging.

Since the early strain gradient theory (Fleck and Hutchinson, 1993 ; 1997 ; Nix and Gao, 1998 ; Gao et al., 1999 ; Huang et al., 2000a ; 2000b ; Qiu et al., 2003) involves higher order stress, the equilibrium equation and boundary conditions are essentially complicated, which cause difficulties to obtain solution. Recently, Huang et al.(2004) proposed a method to obtain the solution of the problem with strain gradient effect included using conventional equilibrium equation and boundary conditions. Huang's method gives an accurate solution except at the very near surface of material as much as the method which involves the complicated equilibrium equation and boundary conditions. As a result, the strain gradient remains in the constitutive equation only.

There are researches that have performed finite element analysis with strain gradient plasticity considered. These can be divided into two groups ; analysis of micro-indentation (Begley and Hutchinson, 1998 ; Shu and Fleck, 1998 ; Huang et al., 2000c) and study of crack initiation and propagation (Xia and Hutchinson, 1996 ; Huang et al., 1999 ; Wei et al., 2004). In their studies, finite element formulation was based on higher-order continuum theory. But those approaches were the displacement-based finite element formulation and hence might be problematic when compressive deformation process such as forging was dealted. When material is forged by a tool (or die), the free surface of material before deformation may come in contact with the tool. This is called 'fold' and one of phenomenon which represents the complexity of non-uniform deformation during forging. Thus, deformation analysis method which overcomes the 'fold' phenomenon and include plastic strain gradient plasticity has been highly disirable.

In this study, we employ the strain gradient plasticity based on conventional continuum theory together with rigid-plastic finite element formulation. Trait of this formulation is that the mesh is updated continuously : Its nodal coordinates during deformation is updated through integration of nodal velocity calculated at each time step. Hence, this method is suitable for the case in which the amount of plastic deformation is very large compared with that of elastic deformation (Kobayashi et al., 1989).

We have examined the plastic deformation behavior of material whose size is 1 μm$\sim$15 μm when the material undergoes a compressive loading. We have used the method of least square to calculate strain gradient at each element during deformation. To reflect the size effect of material, an intrinsic material length parameter together with the concept of strain gradient is included in the constitutive equation. In addition, evolution of geometrically necessary dislocations (GND) dependent on the magnitude of distributed force has been studied.

2. Strain Gradient Plasticity

Development stage of the strain gradient plasticity theory is reviewed briefly and the constitutive equation employed in this study is described.

2.1 Background

Researchers in early stages tried to investigate the size effect phenomenologically through experiment. They carried out torsion, bending and indentation tests, and focused deformation behavior for micrometer-sized and millimeter-sized materials. In classical mechanics viewpoint, the strain (stress) subject to an external loading remains unchanged even though material size is

different. If its size was reduced to fraction of microns, it was proved that the stress in micro-sized material was bigger than that of millimeter-sized material. (Nix, 1989; Stelmashenko et al., 1993; Fleck et al., 1994; Ma and Clarke, 1995; McElhaney et al., 1998; Stolken and Evans, 1998) This is called 'size effect'.

Fleck and Hutchinson (1993; 1997) attributed this size effect to strain gradient which was not considered in the conventional plasticity and developed a higher order equilibrium equation to reflect the size effect. But number of unknowns to be determined increase as the order of equilibrium equation becomes high. Hence, they introduced a parameter 'intrinsic material length' and related it with the unknowns and finally determined the unknowns through experiments. However, the intrinsic material length was not correlated quantitatively with microstructure and/or mechanical property of material, i.e., dislocation density and flow stress.

Nix and Gao (1998) tried to make a quantitative correlation for this parameter and the properties. Using Taylor's dislocation model (Taylor, 1934; 1938), they proposed a flow stress equation that contains the strain gradient and intrinsic material length, and proved its accuracy through micro-indentation test. Gao et al. (1999) extended it to more general type of flow stress equation which includes equivalent strain gradient and intrinsic material length together and proposed Mechanism-based Strain Gradient (MSG) plasticity theory.

MSG theory (Gao et al., 1999; Huang et al., 2000a) still includes, however, higher order equilibrium equation and consequently needs additional boundary conditions to solve the equilibrium equation. Recently, Huang (2004) proposed modified MSG plasticity that does not require higher order equilibrium equation and additional boundary conditions. In this approach, equilibrium equation and boundary condition are the same with those of conventional continuum mechanics. The difference is that the gradient of strain is included in the constitutive equation. This approach has, however, limitation in application to deformation analysis on the very near surface of material.

2.2 Flow stress — dislocation density

Taylor (1934; 1938) expressed the flow stress at continuum level in terms of several parameters at micro level

$$\begin{aligned}\bar{\sigma} &= \bar{M}\bar{\tau} \\ &= \bar{M}\alpha\mu b\sqrt{\rho}\end{aligned} \tag{1}$$

$\bar{M}$, called Taylor factor, represents a conversion factor between critical resolved shear stress, $\bar{\tau}$ of crystalline slip system and the flow stress, $\bar{\sigma}$. In other words, it is a constant which makes the isotropy in continuum level equivalent to the anisotropy of crystal structure. In case of FCC (Face Centered Cubic) metal, $\bar{M}=3.06$ (Huang, 2004). α is material dependent constant and μ, b, ρ represents shear modulus, magnitude of Burgers vector and dislocation density.

The dislocation can be divided into statistically stored dislocation (SSD), ρ_S and geometrically necessary dislocation (GND), ρ_G. Hence, Eq. (1) can be rewritten as followings

$$\bar{\sigma}=\bar{M}\alpha\mu b\sqrt{\rho_S+\rho_G} \tag{2}$$

The concept of SSD and GND was first proposed by Ashby (1970).

2.3 Flow stress — intrinsic material length

If material is deformed statically at room temperature, flow stress, $\bar{\sigma}$ is a function of strain. When material size is reduced up to micrometer, the flow stress is described as a function of strain, strain gradient and intrinsic material length. This is a basic principle of strain gradient plasticity (Huang, 2004) and equation for the flow stress is given in a form

$$\bar{\sigma}=\sigma_{ref}\sqrt{f^2(\bar{\varepsilon})+\chi\bar{\eta}} \tag{3}$$

σ_{ref} and $f(\bar{\varepsilon})$ represents reference stress and work hardening function of the yield stress curve obtained from a tensile test. $\bar{\eta}$ is equivalent strain gradient. χ represents the intrinsic material length and is a parameter which plays a role to make the flow stress dependent upon the material size at micro level.

Difference between characteristic and intrinsic length is explained as followings. In one-dimen-

Table 1 Material constants and intrinsic material length for polycrystalline copper (Qiu et al., 2003)

Material constants	Symbols	Values
Coefficient of the Taylor's dislocation model	α	0.3
Shear modulus	μ	42 [GPa]
Coefficient stress of yield function*	σ_{ref}	688 [MPa]
Magnitude of the Burgers vector	b	0.255 [nm]
Intrinsic material length	χ	1.54 [μm]

* Yield function for polycrystalline copper was 688 $\bar{\varepsilon}^{0.3}$.

sional deformation case, $\chi\bar{\eta}$ in Eq. (3) can be approximated as

$$\chi\bar{\eta}\approx\chi(\Delta\varepsilon/\Delta x)=(\chi/\Delta x)\Delta\varepsilon \tag{4}$$

Δx and χ are, respectively, the characteristic length and intrinsic length of material. When Δx have a similar order compared with χ, $\chi\bar{\eta}$ influences the flow stress behavior. But in case of $\Delta x \gg \chi$, $\chi\bar{\eta}$ in Eq. (4) comes close to zero. Hence, Eq. (3) becomes the flow stress equation usually employed in the conventional plasticity. Huang et al. (2004) suggested an explicit form of χ as follows

$$\chi=\bar{M}\bar{r}\alpha^2\left(\frac{\mu}{\sigma_{ref}}\right)^2 b \tag{5}$$

where $\bar{r}$ is Nye factor which represents average ratio of geometrically necessary dislocation to the most efficient configuration of polycrystalline material. In case of FCC polycrystalline material, $\bar{r}$ is about 1.9. For polycrystalline copper, its mechanical properties and intrinsic material length are listed in Table 1. We know that size of χ is a few micrometers.

2.4 Flow stress in terms of macroscopic and microscopic parameters

To express statistically stored dislocation, ρ_S and geometrically necessary dislocation, ρ_G in an explicit form, we substitute Eq. (5) into Eq. (3). After rearranging it, it is compared with Eq. (2). It yields then an explicit form of statistically stored dislocation and geometrically necessary dislocation as follows

$$\rho_S=\left(\frac{\sigma_{ref}f(\bar{\varepsilon})}{\bar{M}\alpha\mu b}\right)^2 \tag{6}$$

$$\rho_G=\bar{r}\frac{\bar{\eta}}{b} \tag{7}$$

Equation (6) illustrates that the statistically stored dislocation is described in terms of yielding stress ($\sigma_{ref}f(\bar{\varepsilon})$) and shear modulus ($\mu$) which are material parameters defined at continuum level and magnitude of Burgers vector (b) defined at micro level. Meanwhile, Eq. (7) shows that the geometrically necessary dislocation is expressed in terms of parameters at micro level. Beside, it shows that the equivalent strain gradient is a direct measure of geometrically necessary dislocation.

Consequently, the flow stress can be expressed as a function of macroscopic and microscopic parameters. Combination of Eqs. (6), (7) and (2) yields

$$\bar{\sigma}=\bar{M}\alpha\mu b\sqrt{\left(\frac{\sigma_{ref}f(\bar{\varepsilon})}{\bar{M}\alpha\mu b}\right)^2+\bar{r}\frac{\bar{\eta}}{b}} \tag{8}$$

2.5 Strain gradient tensor and equivalent strain gradient

Problem left at this point is to determine the equation for equivalent strain gradient, $\bar{\eta}$. To do this, we begin with definition of strain

$$\varepsilon_{ij}=\frac{1}{2}(u_{i,j}+u_{j,i}) \tag{9}$$

Strain gradient is defined as twice differentiation of displacement field

$$\eta_{ijk}=u_{k,ij} \tag{10}$$

Equation (9) is differentiated until $u_{k,ij}$ is left. If we change the index notation of it properly, Eq. (10) can be then rewritten as

$$\eta_{ijk}=\varepsilon_{ik,j}+\varepsilon_{jk,i}-\varepsilon_{ij,k} \tag{11}$$

Similar to the equivalent strain in the conventional plasticity, the concept of equivalent strain gradient is also introduced. The equivalent strain gradient is expressed in terms of three invariants (Gao et al., 1999).

$$\bar{\eta}=\sqrt{c_1\eta_{iik}\eta_{jjk}+c_2\eta_{ijk}\eta_{ijk}+c_3\eta_{ijk}\eta_{kji}} \tag{12}$$

Application of Eq. (12) to three type of tests, i.e., plane strain bending, pure torsion and axi-symmetric void growth experiment yields algebraic equations in terms of $c_1 \sim c_3$. Solving the algebraic equations give $c_1=0$, $c_2=1/4$ and $c_3=0$. Therefore, the equivalent strain gradient is

$$\bar{\eta}=\sqrt{\frac{1}{4}\eta_{ijk}\eta_{ijk}} \tag{13}$$

2.6 Constitutive equation

In this study, a deformation process where elastic strains are negligible compared with plastic strain is considered. Hence, rigid-plastic constitutive equation is employed. During plastic deformation, increment of strain, $d\varepsilon_{ij}$ is proportional to a deviatoric stress at that instant

$$d\varepsilon_{ij}=d\lambda\sigma'_{ij} \tag{14}$$

$d\lambda$ is a constant proportional to whole deformation process. $\sigma'_{ij}(=\sigma_{ij}-(\sigma_{kk}/3)\,\delta_{ij})$ is deviatoric stress. Using the conventional plasticity, we can get the proportional constant and express deviatoric stress as

$$\sigma'_{ij}=\frac{2\bar{\sigma}}{3\dot{\bar{\varepsilon}}}\dot{\varepsilon}_{ij} \tag{15}$$

$\dot{\varepsilon}_{ij}$ and $\dot{\bar{\varepsilon}}$ represents strain rate tensor and equivalent strain rate. Hence, substituting Eq. (8) into Eq. (15) gives the constitutive equation used in this study.

2.7 Boundary value problem with strain gradient plasticity

Using the strain gradient theory described so far, we can solve following boundary value problem.

- Equilibrium equation :

$$\sigma_{ij,j}+F_d=0 \tag{16}$$

- Constitutive equation :

$$\sigma'_{ij}=\frac{2\dot{\varepsilon}_{ij}}{3\dot{\bar{\varepsilon}}}\left[\bar{M}\alpha\mu b\sqrt{\left(\frac{\sigma_{ref}f(\bar{\varepsilon})}{\bar{M}\alpha\mu b}\right)^2+\bar{r}\frac{\bar{\eta}}{b}}\right] \tag{17}$$

$$\sigma_{ij}=-p\delta_{ij}+\sigma'_{ij} \tag{18}$$

- Incompressibility condition :

$$v_{i,i}=0 \tag{19}$$

- Boundary conditions :

$$\sigma_{ij}n_j=h_i \tag{20}$$

$$v_i=\bar{v}_i \tag{21}$$

F_d represents distributed force vector acting on entire analysis domain. p, h_i and v_i stands for hydrostatic pressure, traction vector and velocity vector of particle. The strain rate tensor, $\dot{\varepsilon}_{ij}$ is related with velocity gradient, i.e., $\dot{\varepsilon}_{ij}=1/2(v_{i,j}+v_{j,i})$. $\dot{\bar{\varepsilon}}$ represents equivalent strain rate and is defined as $\dot{\bar{\varepsilon}}=(2/3\dot{\varepsilon}_{ij}\dot{\varepsilon}_{ij})^{1/2}$.

Equilibrium equation can be rewritten in terms of velocity and hydrostatic pressure by substituting the constitutive equation and the strain rate-velocity relation into Eq. (16). Solving this equation with the boundary conditions, Eqs. (20) and (21) we can obtain velocity and hydrostatic pressure field. The velocity and hydrostatic pressure fields are then substituted for the definition of strain rate, equivalent strain rate and stress.

3. Numerical Implementation

3.1 Plane strain deformation

A plane strain compression problem ($\varepsilon_{zz}=0$) where material size is $1 \sim 15$ μm is taken as an example. Friction between tool and workpiece is assumed tiny and therefore shear strain is negligible ($\varepsilon_{xy}=0$). In this case, since material is deformed plastically, incompressibility condition ($\varepsilon_{xx}+\varepsilon_{yy}=0$) is satisfied. Strain at an element is

$$\varepsilon_{xx}=-\varepsilon_{yy}=\varepsilon \tag{22}$$

The components of the strain gradient are listed in Table 2. From Eq. (13), the equivalent strain

Table 2 Strain gradient tensor for 2-D compression problem

Strain gradient tensors	Strain gradient components	Non-zero terms*
η_{111}	$\varepsilon_{11,1}+\varepsilon_{11,1}-\varepsilon_{11,1}$	$\varepsilon_{,1}$
η_{112}	$\varepsilon_{12,1}+\varepsilon_{12,1}-\varepsilon_{11,2}$	$-\varepsilon_{,2}$
η_{121}	$\varepsilon_{11,2}+\varepsilon_{21,1}-\varepsilon_{12,1}$	$\varepsilon_{,2}$
η_{122}	$\varepsilon_{12,2}+\varepsilon_{22,1}-\varepsilon_{12,2}$	$-\varepsilon_{,1}$
η_{211}	$\varepsilon_{21,1}+\varepsilon_{11,2}-\varepsilon_{21,1}$	$\varepsilon_{,2}$
η_{212}	$\varepsilon_{22,1}+\varepsilon_{12,2}-\varepsilon_{21,2}$	$-\varepsilon_{,1}$
η_{221}	$\varepsilon_{21,2}+\varepsilon_{21,1}-\varepsilon_{22,1}$	$\varepsilon_{,1}$
η_{222}	$\varepsilon_{22,2}+\varepsilon_{22,2}-\varepsilon_{22,2}$	$-\varepsilon_{,2}$

*Note : $\varepsilon_{11}=-\varepsilon_{22}=\varepsilon$ by incompressibility condition and $\varepsilon_{12}=\varepsilon_{21}=0$ from assumption.

gradient for this example is expressed as followings

$$\bar{\eta}=\sqrt{\left(\frac{\partial \varepsilon}{\partial x}\right)^2+\left(\frac{\partial \varepsilon}{\partial y}\right)^2} \tag{23}$$

Equation (23) shows that equivalent strain gradient at an element is a square root of sum of x-direction strain gradient and y-direction one.

To examine the size effect on strain gradient of polycrystalline copper, we design two cases, as shown in Table 3. Case 1 was designed since the intrinsic material length of polycrystalline copper was calculated as 1.54 μm. Case 2, ten times greater than the intrinsic material length, was also taken into account to see the difference when the material size increases significantly beyond the intrinsic material length.

Figure 1 shows finite element meshes before and after deformation, and boundary conditions for two cases. Friction between tool and work-

Table 3 Specimen size and deformation conditions

	Initial height [μm]	Initial width [μm]	Reduction ratio [%]	Die (tool) velocity, v_{Die} [μm/sec]	Friction coefficient	Distributed force, F_d [$\mu N/\mu m^3$]
Case 1	1.54	0.77	30	0.1	0.0	10
Case 2	15.4	7.7	30	0.1	0.0	10

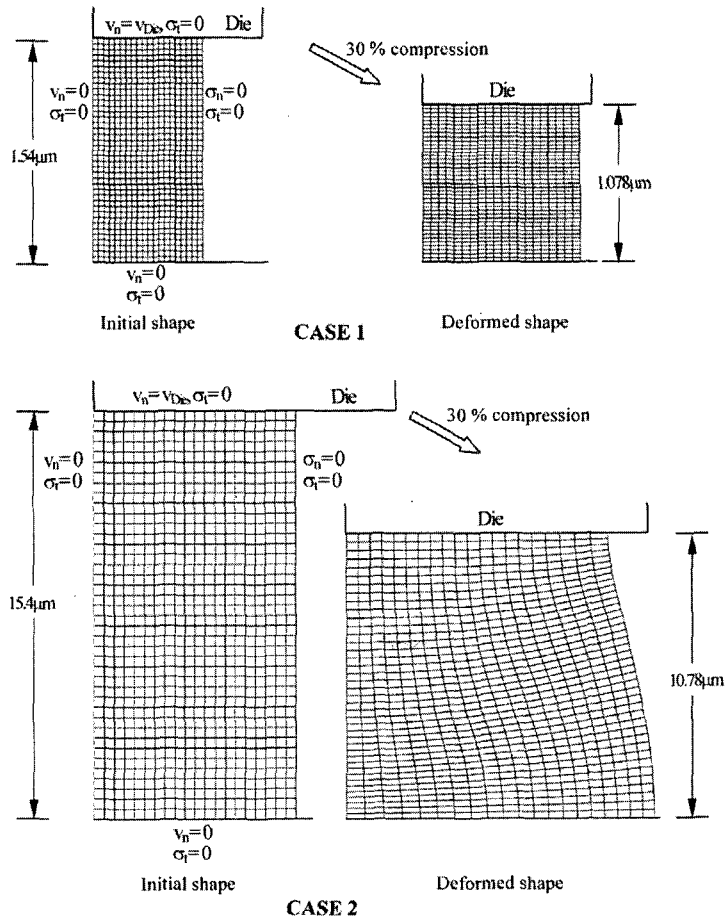

Fig. 1 Boundary conditions and finite element meshes for the two-dimensional compression problem

piece is assumed to be zero. Deformed mesh illustrates no shear deformation since no friction was allowed. We also studied the evolution of stain gradient distribution depending upon a distributed force as well. The distributed force was given to the governing equation in terms of an artificial body force.

3.2 Calculation of element strain

Strain at an element, ε can be determined by substituting Eq. (22) and condition, $\varepsilon_{xy}=0$ into the equivalent strain, $\bar{\varepsilon}=\sqrt{2/3\varepsilon_{ij}\varepsilon_{ij}}$

$$\varepsilon=\frac{\sqrt{3}}{2}\bar{\varepsilon} \tag{24}$$

Equivalent strain for an infinitesimal time step, Δt is updated using following form

$$\bar{\varepsilon}^{(k+1)}=\bar{\varepsilon}^{(k)}+\dot{\bar{\varepsilon}}^{(k+1)}\Delta t^{(k+1)} \tag{25}$$

where $(k+1)$ and (k) represents the time, $t+\Delta t$ and time, t.

3.3 Calculation of element strain gradient

To calculate the strain gradient tensor, i.e. the spatial derivative of strain tensor, we adopted the method of least square. Using this method, we can determine a least square surface, which consists of a corresponding element and elements surrounding it (Fig. 2). It is assumed that the distribution of strain along elements is continuous and does not have a radical change.

The number of elements included in the least square surface is determined by the number of elements surrounding the corresponding element. A set of elements included in the least square surface for the corresponding element is called "element cluster" hereafter. The number of elements in the element cluster is more than nine. If the number of elements is less than nine, an element layer is then added.

As a least square function, we choose a quadratic function as follows:

$$(\tilde{\varepsilon})_m=(\beta_0)_m+(\beta_1)_m x+(\beta_2)_m y+(\beta_3)_m xy+(\beta_4)_m x^2+(\beta_5)_m y^2 \tag{26}$$

where $(\tilde{\varepsilon})_m$ represents the quadratic function at m^{th} element and $(\beta_0)_m\sim(\beta_5)_m$ coefficients. x and y stands for coordinates of the element cluster. It

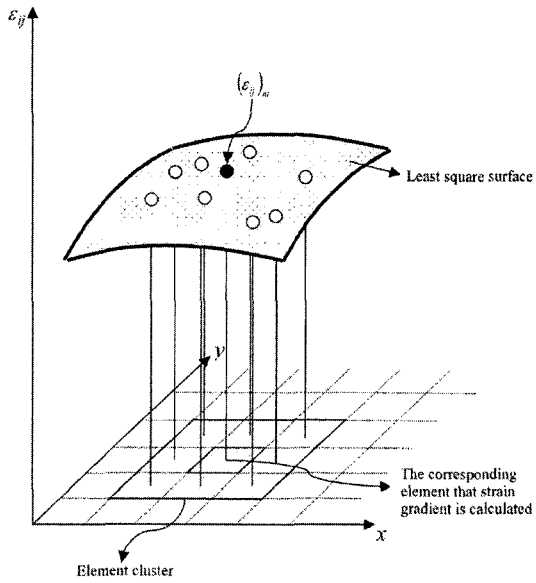

Fig. 2 Schematic diagram of an element cluster and least square function of strain components

is defined the solution of the Eq. (26) to be the coefficient $(\beta_0)_m\sim(\beta_5)_m$ that minimize the sum of the square, Ψ_m

$$\Psi_m=\sum_{i=1}^{n}[(\varepsilon)_i-(\tilde{\varepsilon})_m]^2 \tag{27}$$

where n is the entire number of element in an element cluster and $(\varepsilon)_i$ represents the value for strain in the element cluster. In order for Eq. (27) to be minimum, its partial derivatives with respect to $(\beta_0)_m\sim(\beta_5)_m$, should be equal to zero

$$\frac{\partial\Psi_m}{\partial(\beta_p)_m}=0,\ (p=0,\ 1,\ \cdots,\ 5) \tag{28}$$

Equation (28) is rewritten in a matrix form as followings

$$\begin{bmatrix} n & \sum x_i & \sum y_i & \sum x_iy_i & \sum x_i^2 & \sum y_i^2 \\ & \sum x_i^2 & \sum x_iy_i & \sum x_i^2y_i & \sum x_i^3 & \sum x_iy_i^2 \\ & & \sum y_i^2 & \sum x_iy_i^2 & \sum x_i^2y_i & \sum y_i^3 \\ \text{symm} & & & \sum x_i^2y_i^2 & \sum x_i^3y_i & \sum x_iy_i^3 \\ & & & & \sum x_i^4 & \sum x_i^2y_i^2 \\ & & & & & \sum y_i^4 \end{bmatrix} \begin{bmatrix} (\beta_0)_m \\ (\beta_1)_m \\ (\beta_2)_m \\ (\beta_3)_m \\ (\beta_4)_m \\ (\beta_5)_m \end{bmatrix} = \begin{bmatrix} \sum(\varepsilon)_i \\ \sum x_i(\varepsilon)_i \\ \sum y_i(\varepsilon)_i \\ \sum x_iy_i(\varepsilon)_i \\ \sum x_i^2(\varepsilon)_i \\ \sum y_i^2(\varepsilon)_i \end{bmatrix} \tag{29}$$

Solving Eq. (29) gives the coefficients, $(\beta_0)_m\sim$

$(\beta_5)_m$ and consequently the quadratic function at m^{th} element, i.e., Eq. (26), is fully determined. Finally, the strain gradient at m^{th} element is obtained by differentiating the quadratic function with respect to x and y, respectively

$$(\varepsilon_{,x})_m \approx \frac{\partial(\bar{\varepsilon})_m}{\partial x} = (\beta_1)_m + (\beta_3)_m y + 2(\beta_4)_m x \tag{30}$$

$$(\varepsilon_{,y})_m \approx \frac{\partial(\bar{\varepsilon})_m}{\partial y} = (\beta_2)_m + (\beta_3)_m x + 2(\beta_5)_m y \tag{31}$$

3.4 Computational procedure

In the following, entire procedures which analyze plane strain compression problem using finite element method coupled with the strain gradient plasticity theory are described in detail.

Step (1) Generate finite element mesh and prescribe input parameters and boundary conditions for a given analysis domain.

Step (2) Based on the equivalent strain $(\bar{\varepsilon})$ and equivalent strain gradient $(\bar{\eta})$, compute the flow stress $(\bar{\sigma})$ to evaluate an element stiffness matrix of finite element formulation. For the very first time step, $\bar{\varepsilon}$ and $\bar{\eta}$ are given as input data, which are usually zero.

Step (3) Perform the finite element analysis to obtain nodal velocity as a solution. From the strain rate — velocity relations, calculate strain rate at each element. The details of finite element formulation and computational procedure of this step are well described in the reference, Kobayashi et al., 1989.

Step (4) Update mesh coordinates to be used for next time step, $\mathbf{X}^{(k+1)}=\mathbf{X}^{(k)}+\mathbf{V}^{(k+1)}\Delta t^{(k+1)}$. $\mathbf{X}^{(k+1)}$ and $\mathbf{V}^{(k+1)}$ denote the nodal coordinate and nodal velocity vector at time step $k+1$. $\Delta t^{(k+1)}$ represents the $(k+1)$ *th* time step size. On the basis of the equivalent strain rate $(\dot{\bar{\varepsilon}})$, equivalent strain $(\bar{\varepsilon})$ is computed, $\bar{\varepsilon}^{(k+1)}=\bar{\varepsilon}^{(k)}+\dot{\bar{\varepsilon}}^{(k+1)}\Delta t^{(k+1)}$.

Step (5) To calculate the strain gradient, determine the range of the element cluster. It is based on the nodal connectivity of mesh system used in finite element analysis, as shown in Fig. 2.

Step (6) Apply the method of least square to the elements belonging to the element cluster and obtain the least square function (LSF). The LSF (Eq. (26)) is calculated repeatedly as many as the total number of element included in analysis domain.

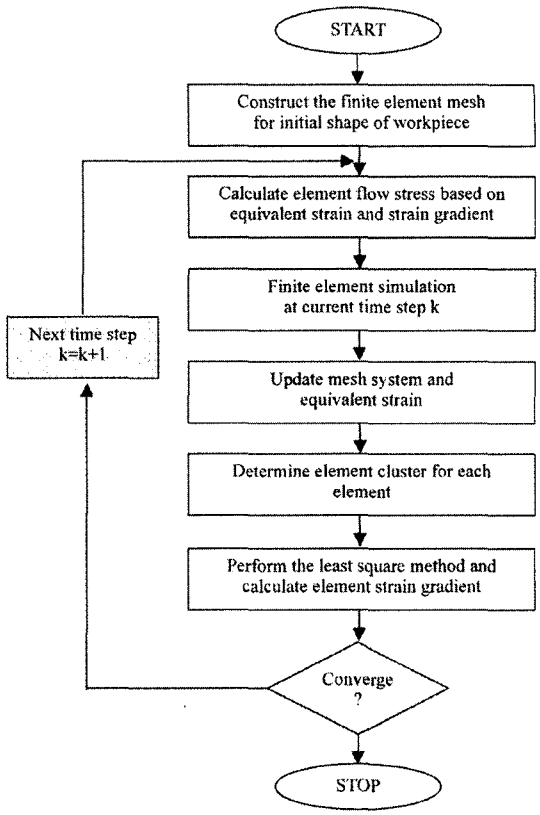

Fig. 3 Flow chart which conducts the finite element analysis coupled with strain gradient plasticity

Step (7) Calculate the strain gradient components through differentiating the least square function with respect to x and y direction. Each element has the two components of strain gradient in this numerical example. Compute the equivalent strain gradient at each element using the Eq. (23).

Step (8) Perform solution process until the amount of loading and/or time step reaches the target. Otherwise, repeat the step (2) ~ (7).

The above steps are su mmarized as a flow chart (Fig. 3).

4. Results and Discussion

Figure 4 shows the distribution of equivalent

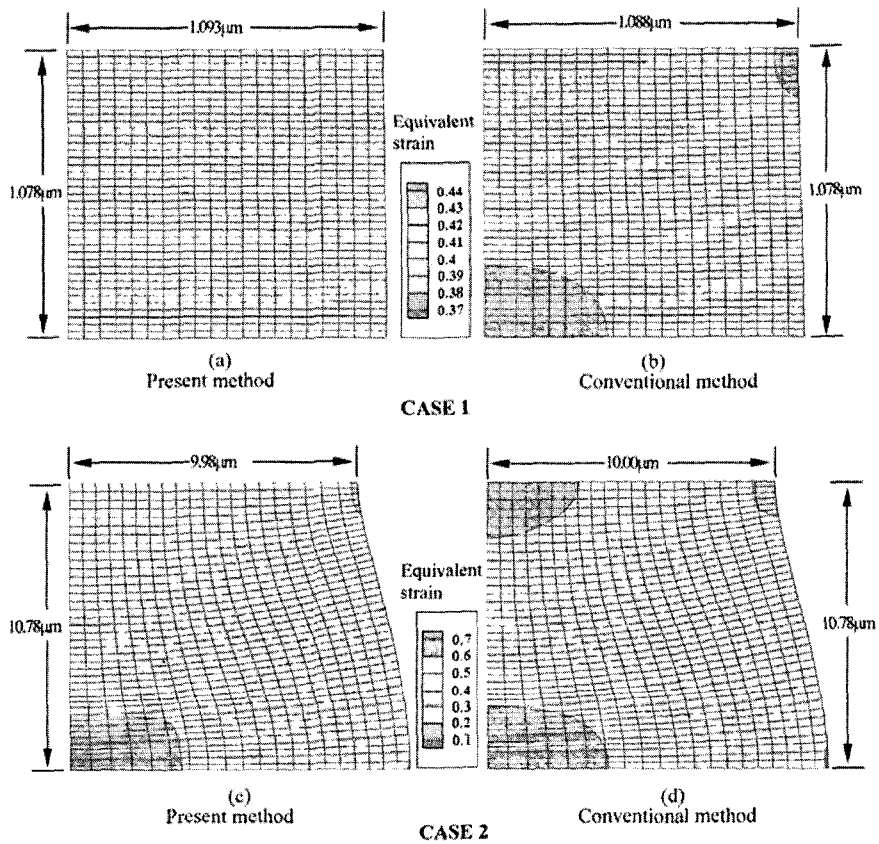

Fig. 4 Distribution of equivalent strain for two cases (See Table 3)

strain for two cases. In Fig. 4(a) and (b), we can observe a distinct difference of equivalent strain distribution when material size is less than the intrinsic material length. Equivalent strain distribution in Fig. 4(a) is very smooth, compared with Fig. 4(b). This indicates when the material size reaches its intrinsic material length, the effect of strain gradient becomes noteworthy and a region where the effect of strain gradient is activated experiences more deformation hardening.

When material size increases significantly like Case 2 (Fig. 4(c) and (d)), on the other hand, the distribution of equivalent strain is almost the same for both methods. These results illustrate clearly the size effect. In other words, both methods (strain gradient plasticity and conventional plasticity) yield almost the same results when the material size is far beyond its intrinsic material length.

It should be noted that lower part of material in Fig. 4(c) and 4(d) underwent a barreling during deformation. This is, however, a deformed shape due to the distributed force applied to the governing equation. Since the material size of Case 2 is 10 times bigger than that of Case 1, the distributed force increases 100 times owing to the increase of acting volume. Subsequently upper part of material pushes its lower part and finally, lower part of material is deformed laterally.

Figure 5 shows the distribution of equivalent strain gradient for two cases. Like the distribution of equivalent strain, the distribution of the equivalent strain gradient with the strain gradient plasticity theory considered is quite different from those with the conventional plasticity theory. In Fig. 5(a) almost no equivalent strain gradient is observed except at the region where the tool contacts material (workpiece). While, in Fig. 5 (b), we can observe some distributions of equivalent strain gradient. Figure 5(c) and (d) also

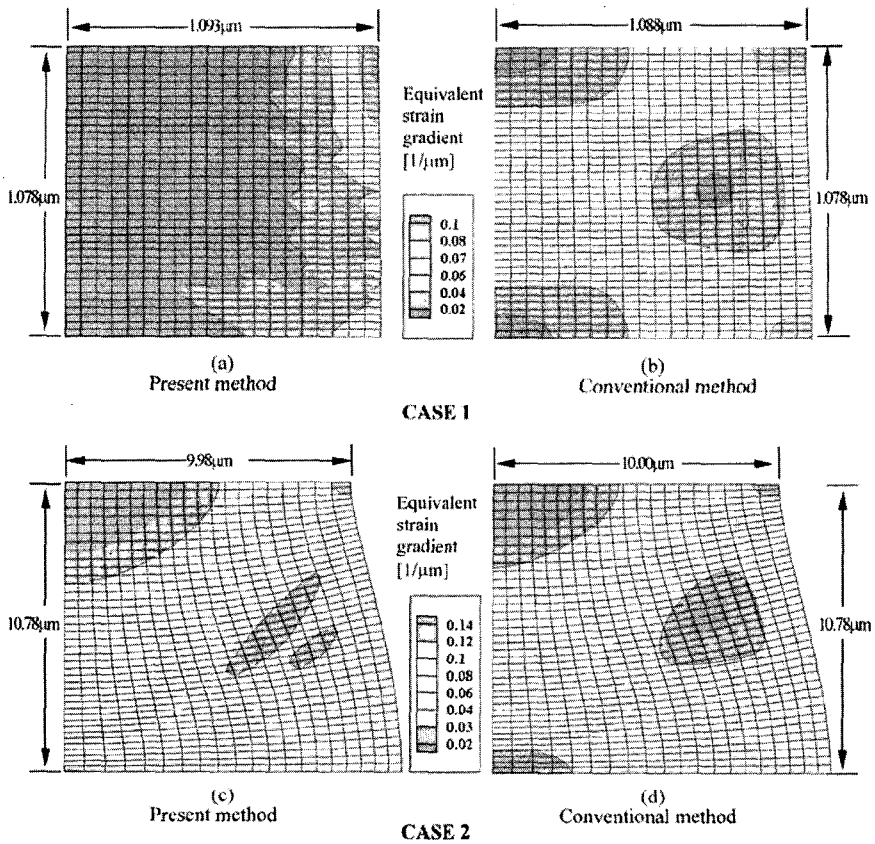

Fig. 5 Distribution of equivalent strain gradient for two cases (See Table 3)

illustrates barreling-like shape due to the distributed force and the increase of acting volume as well. It shows as material size increases the distr -bution of equivalent strain gradient obtained from two methods become similar, as expected.

Figure 6 illustrates the distribution of geometrically necessary dislocation density (GND) for Case 1. Considering the gravitational force of copper is 8.7×10^{-8} $[\mu N/\mu m^3]$, the prescribed distributed force is a very big external force acting on the material. For comparison purpose, such a force is applied to examine the effect of distributed force on GND and subsequently the distribution of strain gradient. Note that GND is directly related with strain gradient (see Eq. (7)). Figure 6(a) shows that when the distributed force is zero, GND density is also almost zero. As the distributed force increases to 5 $[\mu N/\mu m^3]$ and 10 $[\mu N/\mu m^3]$, GND density increases significantly. (Fig. 6(b) and (c)). This indicates the distributed force influences the strain gradient distribution when micrometer-sized material is deformed plastically. Similar to the distribution of equivalent strain gradient, GND density is low at most region of the material. But GND density is large at the corner where tool (die) and material contact each other. Hence, equivalent strain gradient is large at the corner.

Figure 7 shows the equivalent strain — normalized flow stress relation of polycrystalline copper at three points during deformation. Ac, Bc and Cc represents the flow stress calculated by conventional plasticity, and As, Bs and Cs the flow stress calculated by strain gradient plasticity. If we look at the points, Ac, Bc and Cc we can observe that the magnitude of equivalent strain and flow stress at these points are in order. Meanwhile, when the concept of equivalent strain gradient, $\bar{\eta}$ is introduced, the order of the other points (As, Bs and Cs) are changed and those

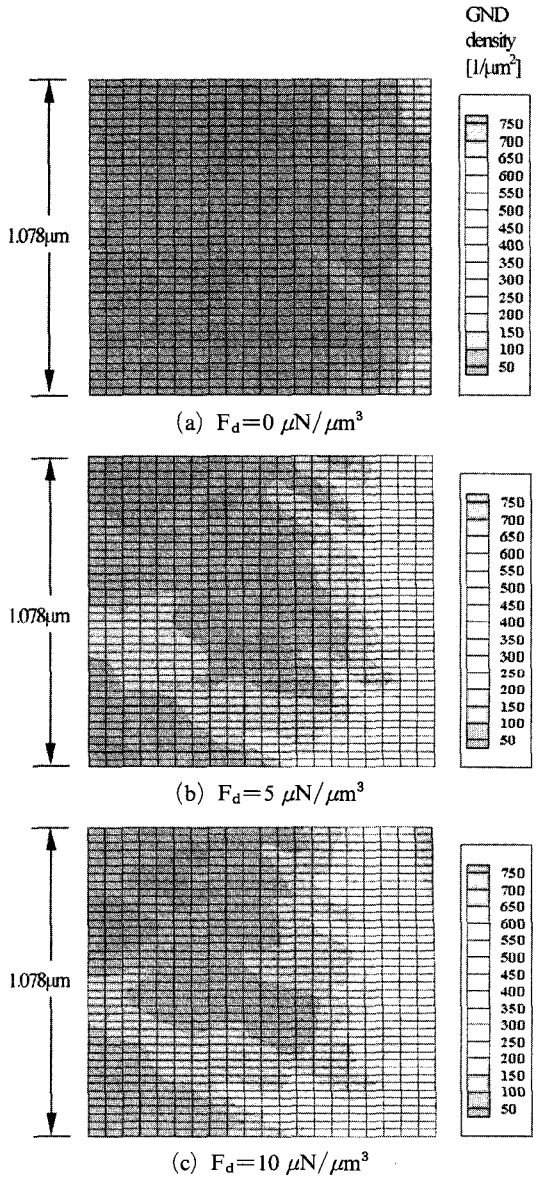

Fig. 6 Geometrically necessary dislocation (GND) density after 30% reduction when different magnitude of distributed force, F_d is applied to CASE 1

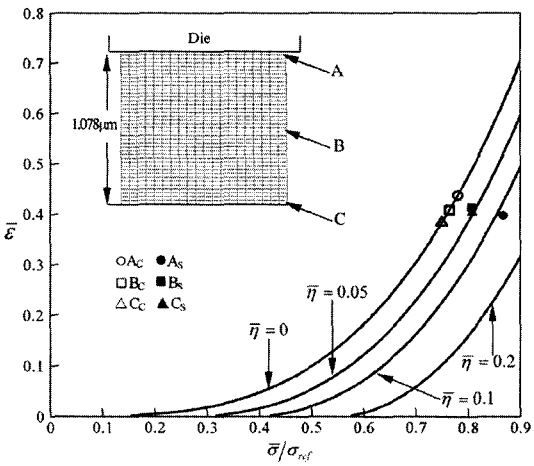

Fig. 7 Reciprocal flow stress curve at each effective strain gradient for the CASE 1. A_C, B_C and C_C represent the flow stress calculated by conventional plasticity at element A, B and C. A_S, B_S and C_S stand for the one calculated by strain gradient plasticity at element A, B and C. The points (A, B and C) move due to introduction of the equivalent strain gradient, $\bar{\eta}$ in the constitutive equation (Eq. (17))

magnitudes are not in order anymore. It is observed that as the strain gradient concept is set up in the constitutive equation, the flow stress at all three points increases. But the path changes of equivalent strain at the points are different. The equivalent strain at points A and B reduced. On the other hand, the one at Point C increases. These behaviors are attributable to the distribution of strain gradient.

5. Concluding Remarks

There have been a lot of efforts to examine the size effect of micro-sized material subject to plastic deformation using the finite element method. These tries were, however, inadequate since the governing equation developed for describing deformation behavior have been used with the material size diminished simply. In this work, we have employed the strain gradient plasticity theory together with finite element method to examine the size effect of micro-sized material. We calculated the strain gradient at each element using the least square function. For demonstrating the size effect during deformation, the finite element method coupled with the intrinsic material length concept has been applied to a plane strain deformation problem.

When material size is less than its intrinsic length the strain gradient becomes significant. If

the material satisfying above condition is deformed plastically, an additional work hardening occurs at the region where the strain gradient effect is noteworthy. This results in a uniform distribution of strain in the material being deformed. This might be a typical phenomenon occurring in the material whose size is less than its intrinsic length. The distributed force influences considerably the distribution of strain gradient. The distributed force magnifies the strain gradient and augments geometrically necessary dislocation density.

The results of this study may contribute to the deformation analysis and design of micro-sized material in the micro-forming, micro-machining and residual stress analysis of micro-electronic packaging.

References

Arsenlis, A. and Park, D. M., 1999, "Crystallographic Aspects of Geometrically Necessary and Statistically Stored Dislocation Density," *Acta Metallurgica et Materialia*, 47, pp. 1597~1611.

Ashby, M. F., 1970, "The Deformation of Plastically Non-homogeneous Alloys," Philosl Mag., 21, pp. 399~424.

Begley, M. R. and Hutchinson, J. W., 1998, "The Mechanics of Size-dependent Indentation," *Journal of Mechanics and Physics of Solids*, 46, pp. 2049~2068.

Fleck, N. A. Muller, G. M. Ashby, M. F. and Hutchinson, J. W., 1994, "Strain Gradient Plasticity: Theory and Experiments," *Acta Metallurgica et Materialia*, 42, pp. 475~487.

Fleck, N. A. and Hutchinson, J. W., 1993, "A Phenomenological Theory for Strain Gradient Effects in Plasticity," *Journal of Mechanics and Physics of Solids*, 41, pp. 1825~1857.

Fleck, N. A. and Hutchinson, J. W., 1997, "Strain Gradient Plasticity," In : J. W. Hutchinson, T. Y. Wu, editors. Advances in applied mechanics. New York : Academic Press., pp. 295~361.

Gao, H., Huang, Y., Nix, W. D. and Hutchinson, J. W., 1999, "Mechanism-based Strain Gradient Plasticity-I. Theory," *Journal of Mechanics and Physics of Solids*, 47, pp. 1239~1263.

Huang, Y., Chen, J. Y., Guo, T. F., Zhang, L. and Hwang, K. C., 1999, "Analytic and numerical studies on mode I and mode II fracture in elastic-plastic materials with strain gradient effects," *International Journal of Fracture*, 100, pp. 1~27.

Huang, Y., Gao, H., Nix, W. D. and Hutchinson, J. W. 2000a, "Mechanism-based Strain Gradient Plasticity-II. Analysis," *Journal of Mechanics and Physics of Solids*, 48, pp. 99~128.

Huang, Y., Qu, S., Hwang, K. C., Li, M. and Gao, H., 2004, "A Conventional Theory of Mechanism-based Strain Gradient Plasticity," *International Journal of Plasticity*, 20, pp. 753~782.

Huang, Y., Xue, Z., Gao, H., Nix, W. D. and Xia, Z. C., 2000b, "A Study of Microindentation Hardness Tests by Mechanism-based Strain Gradient Plasticity," *Journal of Materials Research*, 15, pp. 1786~1796.

Huang, Y., Xue, Z., Gao, H., Nix, W. D. and Xia, Z. C., 2000c, "A Study of Microindentation Hardness Tests by Mechanism-based Strain Gradient Plasticity," *Journal of Material Research*, 15, pp. 1786~1796.

Kobayashi, S., Oh, S. I. and Altan, T., 1989, Metal Forming and The Finite Element Method, Oxford University Press, New York.

Ma, Q. and Clarke, D. R., 1995, "Size Dependent Hardness of Silver Single Crystals," *Journal of Materials Research*, 10, pp. 853~863.

McElhaney, K. W., Vlassak, J. J. and Nix, W. D., 1998, "Determination of Indenter Tip Geometry and Indentation Contact Area for Depth-sensing Indentation Experiments," *Journal of Materials Research*, 13, pp. 1300~1306.

Nix, W. D. and Gao, H., 1998, "Indentation Size Effects in Crystalline Materials : A Law for Strain Gradient Plasticity," *Journal of Mechanics and Physics of Solids*, 46, pp. 411~425.

Nix, W. D., 1989, "Mechanical Properties of Thin Film," *Metallic Transactions*, 20A, pp. 2217~2245.

Qiu, X., Huang, Y., Wei, Y., Gao, H. and Hwang, K. C., 2003, "The Flow Theory of Mechanism-based Strain Gradient Plasticity," *Mechanics of Materials*, 35, pp. 245~258.

Shu, J. Y. and Fleck, N. A., 1998, "The Predic-

tion of a Size Effect in Micro-indentation," *International Journal of Solids and Structures*, 35, pp. 1363~1383.

Stelmashenko, N. A., Walls, M. G., Brown, L. M. and Milman, Y. V., 1993, "Microindentation on W and Mo Oriented Single Crystals: an STM Study," *Acta Metallurgica et Materialia*, 41, pp. 2855~2865.

Stolken, J. S. and Evans, A. G., 1998, "A Microbend Test Method for Measuring the Plasticity Length Scale," *Acta Metallurgica et Materialia*, 46, pp. 5109~5115.

Taylor, G. I., 1934, "The Mechanism of Plastic Deformation of Crystals. Part I — Theoretical," *Proceedings of the Royal Society of London A*, 145, pp. 362~387.

Taylor, G. I., 1938, "Plastic Strain in Metals," *Journal of the Institute of Metals*, 62, pp. 307~324.

Wei, Y., Qiu, X. and Hwang, K. C., 2004, "Steady-state Crack Growth and Fracture Work based on the Theory of Mechanism-based Strain Gradient Plasticity," *Engineering Fracture Mechanics*, 71, pp. 107~125.

Xia, Z. C. and Hutchinson, J. W., 1996, "Crack Tip Fields in Strain Gradient Plasticity," *Journal of Mechanics and Physics of Solids*, 44, pp. 1621~1648.